UC Davis

San Francisco Estuary and Watershed Science

Title

Use of the SmeltCam as an Efficient Fish-Sampling Alternative Within the San Francisco Estuary

Permalink

https://escholarship.org/uc/item/39k1772k

Journal

San Francisco Estuary and Watershed Science, 19(2)

Authors

Huntsman, Brock M.
Feyrer, Fredrick
Young, Matthew J.

Publication Date

2021

DOI

10.15447/sfews.2021v19iss2art6

Supplemental Material

https://escholarship.org/uc/item/39k1772k#supplemental

Peer reviewed

RESEARCH

Use of the SmeltCam as an Efficient Fish–Sampling Alternative within the San Francisco Estuary

Brock M. Huntsman*[1], Frederick Feyrer[1], Matthew J. Young[1]

ABSTRACT

Resource managers often rely on long-term monitoring surveys to detect trends in biological data. However, no survey gear is 100% efficient, and many sources of bias can be responsible for detecting or not detecting biological trends. The SmeltCam is an imaging apparatus developed as a potential sampling alternative to long-term trawling gear surveys within the San Francisco Estuary, California, to reduce handling stress on sensitive species like the Delta Smelt (*Hypomesus transpacificus*). Although believed to be a reliable alternative to closed cod-end trawling surveys, no formal test of sampling efficiency has been implemented using the SmeltCam. We used a paired deployment of the SmeltCam and a conventional closed cod-end trawl within the Napa River and San Pablo Bay, a Bayesian binomial *N*-mixture model, and data simulations to determine the sampling efficiency of both deployed gear types to capture a Delta Smelt surrogate (Northern Anchovy, *Engraulis mordax*) and to test potential bias in our modeling framework. We found that retention efficiency—a component of detection efficiency that estimates the probability a fish is retained by the gear, conditional on gear contact—was slightly higher using the SmeltCam (mean = 0.58) than the conventional trawl (mean = 0.47, Probability SmeltCam retention efficiency > trawl retention efficiency = 94%). We also found turbidity did not affect the SmeltCam's retention efficiency, although total fish density during an individual tow improved the trawl's retention efficiency. Simulations also showed the binomial model was accurate when model assumptions were met. Collectively, our results suggest the SmeltCam to be a reliable alternative to sampling with conventional trawling gear, but future tests are needed to confirm whether the SmeltCam is as reliable when applied to taxa other than Northern Anchovy over a greater range of conditions.

KEY WORDS

INTRODUCTION

Nearly all sampling methods in fisheries and wildlife are imperfect (Royle et al. 2005). Not detecting an individual during a survey does not

exclusively mean a species is absent, but may reflect whether the species was available to or retained by the chosen gear. Such imperfections in the observation process propagate into the desired latent state metric (e.g., abundance, survival, diversity) that a study is designed to estimate. Although this source of bias can dramatically alter inference if unaccounted for (Kéry and Royle 2016), implementing appropriate sampling designs that can address catchability issues is not trivial.

In fisheries, the common catch equation explicitly defines the issue of detection efficiency (Catch = Detection Efficiency × Fishing Effort × Latent State Abundance, Walsh 1997). Detection efficiency can be further decomposed into components, which vary because of differing sources of sampling bias (Zhou et al. 2014; Hostetter et al. 2019). The common components of detection efficiency are the probability that a fish is present during sampling; the probability the fish, given it is present, is available to the gear; and the probability that a fish is retained once in contact with the gear, or retention probability (Hostetter et al. 2019; Vasilakopoulos et al. 2020). Various sampling designs have been developed to specifically target components of sampling efficiency (e.g., retention probability with covered cod-end trawling designs) or combinations of detection efficiency components (e.g., depletion surveys provide information specific to retention and availability probability, Hostetter et al. 2019). Often such sampling designs require replicate samples to be collected during demographic closure (i.e., when no movement, births, or deaths are occurring, Nichols et al. 2009; Amundson et al. 2014; Zhou et al. 2014), providing the appropriate sampling design to estimate bias in sampling efficiency. Designing experiments where closure is certain is relatively simple when surveys occur within small water bodies (e.g., using block nets within wadeable streams); however, it is difficult to ensure demographic closure in larger water bodies (large rivers, lakes, estuaries), and creative solutions are required. This difficulty is exacerbated for species with conservation status, especially if the most efficient gear types coincide with adverse effects (e.g., greater fish mortality when electrofishing or trawling).

The upper San Francisco Estuary (the estuary) provides municipal and agricultural water to satisfy most of California's freshwater demand, and is also home to multiple listed species that are dependent on this water supply. The Delta Smelt (*Hypomesus transpacificus*) is a federally threatened fish species (CDFW 2020) that is often the focus for resource managers tasked with balancing ecological needs and human demands because its decline is linked in part to freshwater outflows (Kimmerer and Rose 2018). A major concern with monitoring Delta Smelt populations is that it is sensitive to sampling mortality when collected by standard methods within the estuary (conventional trawls), and few sampling alternatives are currently available that can provide equally reliable indices of abundance (Feyrer et al. 2013). Recently, Feyrer et al. (2013) showed that an underwater video camera attached to trawling gear, referred to as the SmeltCam, could not only detect fish passing through the trawl but also reduced mortality by removing the need to handle fish (although some fish do get entangled in the mesh). The SmeltCam has been used to investigate the distribution of pelagic communities within different habitats of the estuary (Feyrer et al. 2017), suggesting its effectiveness to monitor taxa other than the fish species for which it was designed. Although current evidence points to the SmeltCam as a valid alternative to conventional trawling methodologies, no formal assessment of gear detection efficiency has been conducted.

Paired gear sampling designs can be used to assess detection efficiency among sampling gears in fisheries studies (Walsh 1997; Millar and Fryer 1999) and can be used to assess the relative efficiency of the SmeltCam as a sampling alternative to conventional trawling methods. For example, Coggins Jr. et al. (2014) combined baited traps and video cameras to estimate imperfect detection within an occupancy modeling framework. An important aspect of the paired gear sampling design is that the paired gear deployments simultaneously act as replicate, closed sampling passes (Coggins Jr. et al. 2014), a requirement for studies designed to estimate detection bias in sampling methods. Retention

probability—the probability that an organism is retained by the sampling gear, conditional on it being available to the gear—is a component of detection efficiency commonly estimated for trawling gear deployed in the estuary. Paired gear studies have already been conducted within the estuary to estimate gear retention probability for Delta Smelt (Mitchell et al. 2017, 2019) and used to provide a less biased index of abundance throughout the estuary (Polansky et al. 2019). However, no such assessment has been performed for the SmeltCam, which is important if it is to be used as a viable alternative to conventional trawling surveys.

The goal of this study was to assess the gear retention efficiency of the SmeltCam relative to conventional trawling surveys deployed within the estuary. We used a paired gear sampling design, with the SmeltCam deployed simultaneously with a conventional trawl that targeted Northern Anchovy (*Engraulis mordax*) as a Delta Smelt surrogate to test the relative retention efficiency of the SmeltCam compared with conventional trawling methods. Our specific objectives were to (1) estimate how common environmental conditions during sampling might affect retention efficiency of the SmeltCam and a conventional trawl, (2) compare retention efficiency of the sampling gear types, and (3) use data simulations to determine potential bias in paired gear retention efficiency analyses.

MATERIALS AND METHODS
Field Data Collection
We performed our study in September of 2016 within the Napa River and San Pablo Bay, California (Figure 1). Surveys were conducted using the same equipment and operating protocols as normally deployed by the California Department of Fish and Wildlife (CDFW) during Fall Midwater Trawl (FMWT) surveys (Feyrer et al. 2007, 2013; *https://www.dfg.ca.gov/delta/data*), and near fixed sampling stations sampled by CDFW monitoring programs (Napa River stations 340 and 341; San Pablo Bay stations 310 and 311; *https://www.dfg.ca.gov/delta/data/fmwt/stations.asp*). The net is 3.66 m in width and height, and

17.6 m long, with nine tapered panels of stretch mesh that start at 14.7 cm near the mouth to 1.3 cm in the cod end.

The SmeltCam is a video camera apparatus (Genie HM1400, Teledyne Dalsa) attached to the cod end of a midwater trawl (see Feyrer et al. 2013 for more details about the SmeltCam's design). The purpose of the trawl-camera's design is to function as an open-ended trawling system in which fishes can be identified by trawling methods without the need to bring fish to the surface and retrieve them from a closed cod end (Feyrer et al. 2013). Unlike previous studies (Feyrer et al. 2013, 2017), we included a closed cod end with the SmeltCam for our sampling design to test the fish retention efficiency of the SmeltCam relative to a typical oblique tow. Thus, our methods are similar to Coggins Jr. et al. (2014) in that the paired gear deployment served as replicate surveys in which gear retention efficiency could be assessed.

We conducted 65 paired SmeltCam and closed cod-end oblique tows over 4 sampling days, with each tow lasting roughly 12 minutes. All tows occurred against the current, 35 within the Napa River and 30 within San Pablo Bay. For analysis, we removed data points with missing covariate information, which reduced the number of tows to 52 (Napa River, $n = 26$; San Pablo Bay, $n = 26$). We conducted tows from 9/15/2016 to 9/16/2016 within the Napa River, and from 9/22/2016 to 9/23/2016 within San Pablo Bay, where the time between tows ranged from 17 minutes to 253 minutes. We estimated the volume of water filtered by the net using a mechanical flowmeter (model 2030R, General Oceanics) deployed off the side of the vessel during tows, with calculations provided by the manufacturer to account for tow speed and net size. We used a hand-held EXO2 YSI multi-parameter sonde (YSI Inc.) to determine water temperature (°C), turbidity (NTU), specific conductivity (μS cm^{-1}), and salinity (ppt); and a boat-mounted sonar unit to estimate water depth (m) after tows were completed.

We counted Northern Anchovy separately for the SmeltCam and the cod end. For the SmeltCam, all
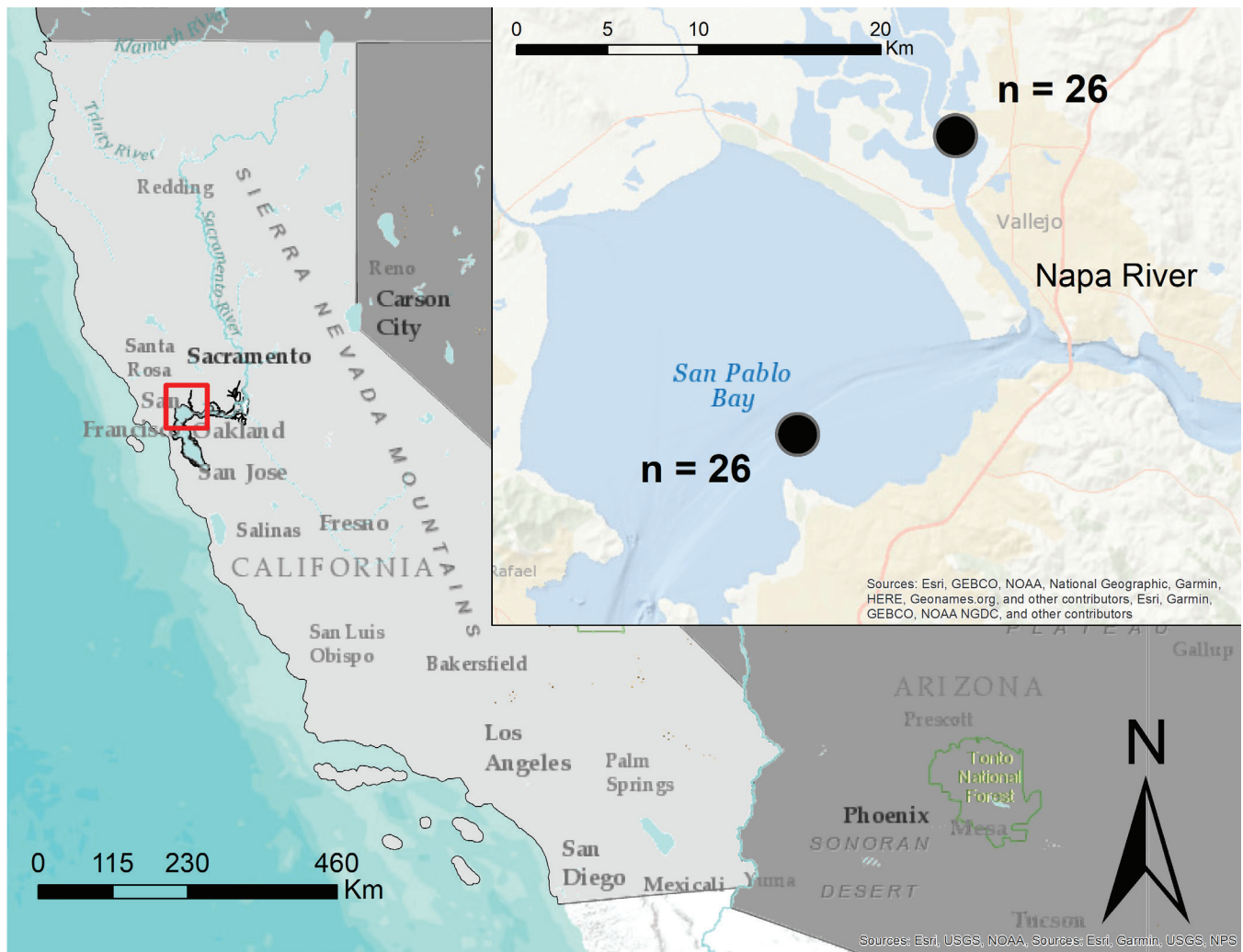
Figure 1   Sampling locations (*black circles*) within San Pablo Bay and the Napa River, San Francisco Estuary, California

images were processed by an expert in the lab, where fish were identified and counted. All fishes caught in the cod end were identified and counted in the field.

Statistical Analyses

We used a binomial *N*-mixture modeling approach (Royle 2004) to analyze the combined trawl–SmeltCam data to test for differences in retention efficiency between the two gear types. We used the dual gear binomial *N*-mixture modeling approach described by Graves et al. (2011) to analyze our data set, where two binomial *N*-mixture models were fit to count data collected by separate sampling methods within the same sampling area. This modeling approach assumes

that latent state abundance (*N*) in contact with the gear was the same, regardless of sampling gear used, but differences in the observation process between gear types is the primary source of variability. We fit this same model with our dual gear surveys for Northern Anchovy with the following form:

(1)

$$y_{Camera_i} \sim Binomial\left(N_i, p_{Camera_i}\right)$$

$$logit\left(p_{Camera_i}\right) = \alpha_{Camera} + \beta_{Camera_{Turbidity}} * Turbidity_i + \varepsilon_{Camera_i}$$

$$\varepsilon_{Camera_i} \sim Normal\left(0, \sigma^2_{Camera}\right)$$

(2)

$$y_{Trawl_i} \sim Binomial\left(N_i, p_{Trawl_i}\right)$$

$$logit\left(p_{Trawl_i}\right) = \alpha_{Trawl} + \beta_{Trawl_{Density}} * Density + \varepsilon_{Trawl_i}$$

$$\varepsilon_{Trawl_i} \sim Normal\left(0, \sigma_{Trawl}^2\right)$$

where

$$N_i \sim Poisson(\lambda_i)$$

$$\log(\lambda_i) = \alpha_N + \log\left(Volume_i\right) + \beta_{N_{Flood}} * \beta_{N_{HighSlack}} * HighSlack_i$$

$$+ \beta_{N_{LowSlack}} * LowSlack_i + \beta_{N_{SanPablo}} * SanPablo_i + \varepsilon_{N_i}$$

and y is observed counts of Northern Anchovy from the SmeltCam (*Camera*) and the number of Northern Anchovy captured in the closed cod end of the trawl (*Trawl*) during each individual tow (*i*). Gear-specific retention efficiency (*p*) was constrained as a function of turbidity for the SmeltCam because of its presumed effect on video processing (DeCelles et al. 2017). The retention efficiency of the closed cod end was modeled as a function of the log-transformed total number of fish (plus 1 due to zeros) captured in the sample, because this is known to increase the sampling efficiency of trawl surveys because it blocks the mesh from which smaller fish may escape (Mitchell et al. 2017; Peterson and Barajas 2018). The latent state abundance parameter was also constrained by fixed tide effects (β_i; ebb, flood, high slack, low slack) and site effects (Napa River vs. San Pablo Bay), with the intercept (α_N) representing the ebb tide within the Napa River. We included the log transformation of the volume of water filtered during individual trawls as an offset. We also included a random effect (ε) for each observation in the observation process (p_{Camera_i} and p_{Trawl_i}), and the latent state process (N_i) to account for over-dispersion (Kéry 2010; Harrison 2014), with σ as observation-level standard deviations.

We fit the dual gear *N*-mixture model using a Bayesian framework, with minimally informative priors assigned to all model parameters (Table 1). We conducted full Bayesian inference using Gibbs sampling (JAGS v4.3.0; Plummer et al. 2017) via Markov Chain Monte Carlo (MCMC) sampling

with the jagsUI package in program R (Kellner 2019; R Core Team 2020). Final inferences for the *N*-mixture model were based on 6,000 samples for each parameter from the posterior distributions. Posteriors were generated from three independent chains, each with an initial length of 110,000 iterations, burn-in of 10,000 and a thinning of 50. We assessed model convergence by examining Gelman and Rubin convergence diagnostics ($\hat{R} < 1.1$; Gelman and Rubin 1992). We assessed "goodness-of-fit" for the *N*-mixture model by calculating a χ^2 discrepancy and a Bayesian *p*-value to assess model fit (Kéry and Royle 2016). Bayesian *p*-values indicate poor fit near values of 0 and 1, with the best fit at values near 0.5. Because the SmeltCam and the conventional trawl data were fit with two separate binomial *N*-mixture models integrated by a shared latent state abundance parameter, we assessed model fit by calculating a separate χ^2 discrepancy for the SmeltCam and conventional trawl observation processes (gear retention efficiency).

We used two criteria as evidence for Objectives 1 and 2. We designated parameters with 95% credible intervals that did not overlap 0 as evidence for environmental conditions that affected retention efficiency of both gear types and latent state abundance (Objective 1). Objective 2 was addressed in multiple steps. First, we predicted retention efficiency for each tow from both gear types. We took the mean from all tows, which resulted in a retention efficiency estimate for each gear type and posterior sample. We then compared retention efficiency predictions of the SmeltCam to closed cod-end midwater trawl predictions. We used the probability of direction to determine whether retention efficiency differences existed between the SmeltCam and the conventional trawl from posterior samples [Pr(Camera > Trawl)]; Makowski et al. 2019). If 95% of retention efficiency posterior samples were greater for one gear type than the other, we considered this evidence of an effect. Lastly, we used the probability of direction to also determine whether differences existed [Pr(Camera > Trawl)] based on the intercept estimates for each retention efficiency model (α_{Camera} and α_{Trawl}). We used this criterion because the intercept represents the

Table 1 Model priors and posterior parameter estimates fit to the integrated binomial *N*-mixture model with SmeltCam and midwater trawl sampling gears in the San Francisco Estuary, California. Parameters reflect notation presented in Equations 1 and 2. Posterior values are means, with 95% credible intervals reported in parentheses. *Bold numbers* represent parameters with 95% credible intervals that did not overlap 0. The σ parameters could not overlap 0 because standard deviations can't be less than 0.

Process	Parameter	Definition	Prior	Posterior
Observation				
	α_{Camera}	Camera intercept	Normal (0, 10)	0.44 (-0.46, 1.65)
	$\beta_{Turbidity}$	Camera turbidity effect	Normal (0, 10)	0.30 (-0.34, 1.09)
	σ_{Camera}	Camera random observation effect	Uniform (0, 100)	0.80 (0.04, 2.38)
	α_{Trawl}	Trawl intercept	Normal (0, 10)	−1.25 (−2.99, 0.60)
	$\beta_{Density}$	Trawl density effect	Normal (0, 10)	**0.63 (0.07, 1.33)**
	σ_{Trawl}	Trawl random observation effect	Uniform (0, 100)	1.56 (0.57, 3.11)
Latent State				
	α_N	Intercept (ebb tide and Napa River)	Normal (0, 100)	**−7.54 (−8.80, −6.37)**
	$\beta_{N_{Flood}}$	Flood tide effect	Normal (0, 100)	**−1.93 (−3.31, −0.63)**
	$\beta_{N_{High\ Stack}}$	High slack tide effect	Normal (0, 100)	**−2.64 (−4.60, −0.81)**
	$\beta_{N_{Low\ Stack}}$	Low slack tide effect	Normal (0, 100)	−0.89 (−3.35, 1.65)
	$\beta_{N_{San\ Pablo}}$	San Pablo Bay effect	Normal (0, 100)	**1.57 (0.40, 2.83)**
	σ_N	Random observation effect	Uniform (0, 100)	1.85 (1.30, 2.62)
Model Fit				
	Bayesian *p*	Camera data	—	0.53
	Bayesian *p*	Trawl data	—	0.45

expected mean of retention efficiency for each gear type when standardized covariates equal 0.

Simulations

We performed data simulations to test whether the model provided unbiased estimates of gear efficiency (Objective 3, see Appendix A for R code). We simulated data with linear constraints on the observation process (retention efficiency of the SmeltCam and trawl) and the latent state process (abundance), similar to the analytical framework described in Equations 1 and 2 but without the random observation effect, which was included to improve model fit for the observed data. The binomial model simulations included scenarios in which the intercept of both the SmeltCam and the trawl retention efficiencies were set at three different values (back-transformed from the logit scale = 0.4, 0.6, and

0.8) for a total of nine mean retention efficiency scenarios between the SmeltCam and trawl surveys.

The purpose of these simulation scenarios was to determine the extent that mean gear retention efficiency affected model reliability. We included a negative covariate effect (–1.0) for the SmeltCam simulation, which was the assumed effect of turbidity on SmeltCam retention efficiency. A positive effect also was included for the trawl retention efficiency simulation (1.0), an assumed effect of fish density on the retention efficiency of the trawling gear (Mitchell et al. 2017). A second simulation scenario included a range of sample sizes (or sites) to determine whether our sample size of 52 tows was sufficient to produce unbiased results of gear efficiency and how many tows (*n* = 25, 52, 88, 150) would be needed to

produce reliable parameter estimates. A final simulation scenario included additional replicate passes during closed sampling for both gear types, which is similar to conventional occupancy and binomial *N*-mixture model sampling designs (Royle et al. 2005). The replicate pass scenario included either a single pass with both gear types (like the current Northern Anchovy analysis), three passes, or six passes. In all simulations, the latent state parameter was fit with linear constraints, with an intercept set at 2.7 [log(15) = 2.7, and the mean observed counts were 13 and 14 for trawl and SmeltCam, respectively], with a slope set at 2. A total of 10,800 simulations were run (100 simulations × four site scenarios × three camera efficiency scenarios × three trawl efficiency scenarios × three replicate sample scenarios). When a simulation did not converge ($\hat{R}$ of all parameters < 1.1), additional simulations were performed until 100 converged simulations were gained. We assessed model performance for all parameters of each simulation scenario for 100 converged simulations (Zhao and Royle 2019). We assessed model performance by calculating relative bias ($\frac{Median\,Estimate - Truth}{Truth}$; Amundson et al. 2014;

Duarte et al. 2018), whether the truth was captured by 95% credible intervals (coverage; Amundson et al. 2014), and assessed for accuracy

with root-mean-squared error (RMSE = $\sqrt{\frac{\sum(Median\,Estimate - Truth)^2}{Number\,of\,Simulations}}$; Walther and Moore 2005; Hostetter et al. 2019). Models were similarly fit with Bayesian approaches but with 11,000 iterations, 1,000 samples removed (burn-in), a thinning of five, and three chains run in parallel.

RESULTS

Northern Anchovy counts and habitat variables collected during trawling surveys varied between sampling locations. The highest number of Northern Anchovy captured with either gear type occurred in San Pablo Bay, where mean observed counts were approximately 8 to 12 times higher than counts from the Napa River (Table 2). Northern Anchovy counts were similar between gear types on each individual tow, although some variability was evident (Figure 2). Water-quality measurements also differed among sampling locations, with greater conductivity and salinity in San Pablo Bay, and all other measured water-quality variables higher in the Napa River (Table 2).
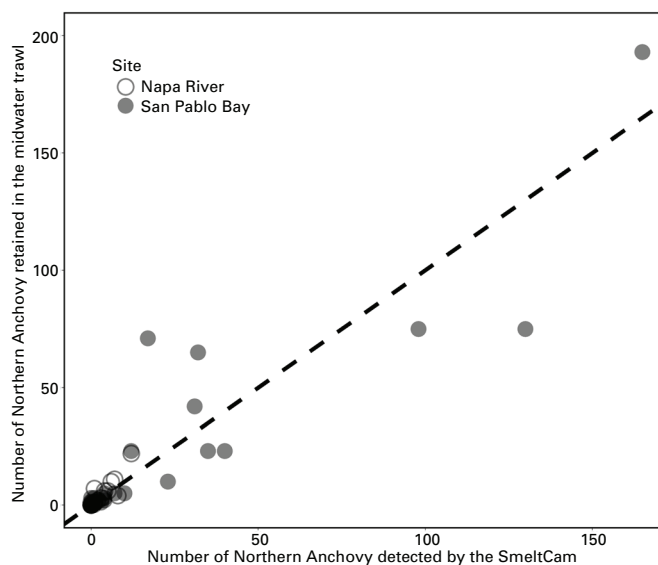
Table 2 Sampling conditions during dual gear surveys in the San Francisco Estuary, California. All values reported for continuous habitat and sampling condition variables are means (SE). The Northern Anchovy counts from the SmeltCam and Trawl are reported as means with minimums and maximums in parentheses.

Variable	Napa River	San Pablo Bay
SmeltCam counts	3.0 (0, 22)	24.2 (0, 193)
Trawl counts	2.0 (0, 12)	23.8 (0, 165)
Volume	8,853 (402)	10,383 (590)
Turbidity (NTU)	22.4 (1.6)	10.8 (1.5)
Conductivity (µS cm^{-1})	32,022 (232)	42,464 (395)
Salinity (ppt)	20.0 (0.2)	27.4 (0.3)
Temperature (° C)	19.3 (0.1)	18.5 (0.1)
Depth (m)	13.5 (0.1)	13.2 (0.2)

Figure 2 Observed Northern Anchovy counts detected with the SmeltCam vs. the closed cod end of the midwater trawl during dual gear surveys in the San Francisco Estuary, California. The *broken red line* represents a 1:1 relationship
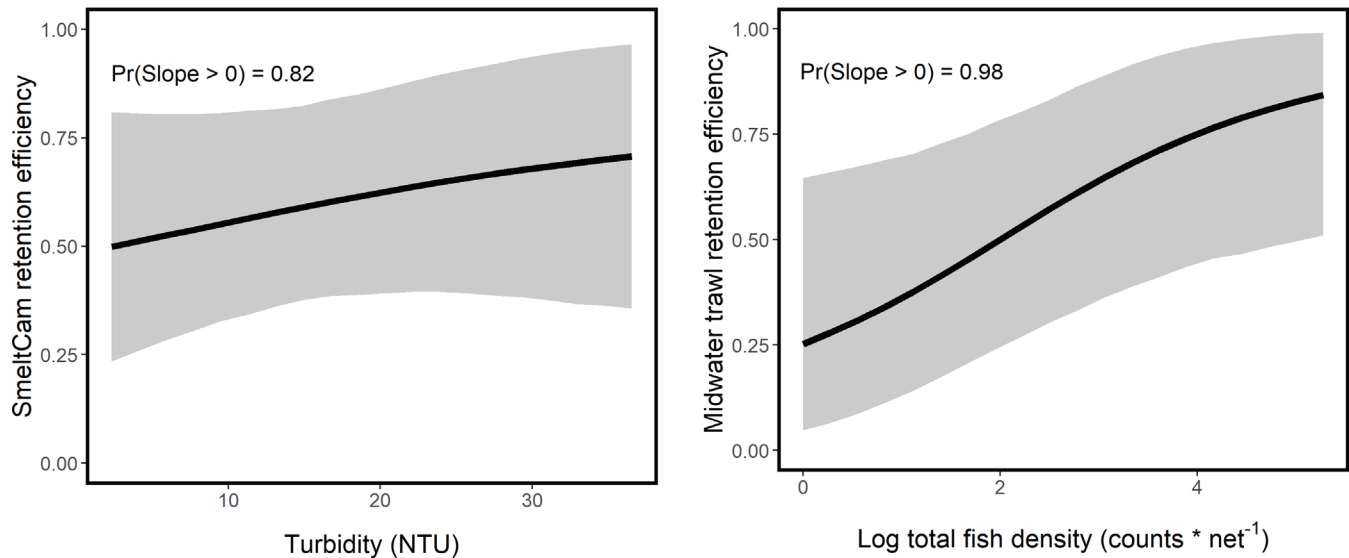
Figure 3 Turbidity and log transformed total fish density effects on Northern Anchovy retention efficiency using the SmeltCam and closed cod-end midwater trawl sampling gears, respectively

Objective 1

Analysis of the Northern Anchovy data with the integrated binomial N-mixture model showed adequate model fit (Bayesian $p = 0.53$ and 0.45 for the camera data and trawl data respectively, Table 1). No evidence was found that turbidity affected SmeltCam retention efficiency (Table 1), where 18% of the posterior samples for the turbidity effect were less than 0, and 95% credible intervals overlapped 0 (mean $\beta_{Turbidity} = 0.30$, 95% credible intervals = −0.34 to 1.09; Figure 3). Retention efficiency of the trawl increased with fish density (Table 1), with 98% of the posterior samples for the fish density effect greater than 0, and 95% credible intervals did not overlap 0 (mean $\beta_{Density} = 0.63$, 95% credible intervals = 0.07 to 1.33; Figure 3).

Northern Anchovy were also more abundant during ebb tide than either flood tide (mean $\beta_{N_{Flood}} = -1.93$, 95% credible intervals = −3.31 to −0.63) or high slack tide (mean $\beta_{N_{High\ Stack}} = -2.64$, 95% credible intervals = −4.60 to −0.81; Table 1). Northern Anchovy abundance during ebb tide was not different than at low slack tide (mean $\beta_{N_{Low\ Stack}} = -0.89$, 95% credible intervals = −3.35 to 1.65; Table 1 and Figure 4).
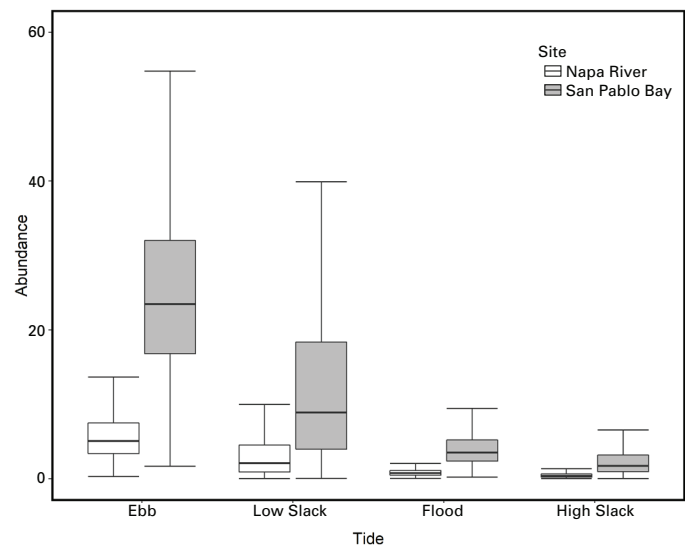

Figure 4 Predicted latent state abundance by sampling location and tidal phase from simultaneous SmeltCam and midwater trawl surveys of Northern Anchovy in the San Francisco Estuary, California

Objective 2

Multiple analyses estimated retention efficiency to be higher for the SmeltCam than the closed cod-end (trawl). Overall mean retention efficiency for the SmeltCam was higher than the closed cod end based on all 52 tows, with 94% of posterior samples (mean retention efficiency = 0.58, 95%
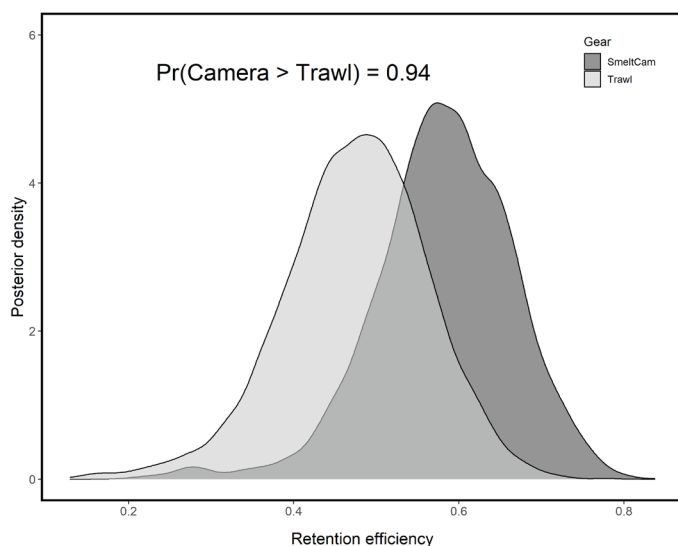
Figure 5 Posterior density of the mean retention efficiency using the combined SmeltCam and closed cod-end midwater trawl (Trawl) sampling gears analyzed with the integrated binomial N-mixture model

credible intervals = 0.40 to 0.73) greater than posterior samples of retention efficiency for the closed cod end (mean retention efficiency = 0.47, 95% credible intervals = 0.28 to 0.64; Figure 5). Similar results were found when we compared the retention efficiency intercepts, where 97% of posterior samples were higher for the SmeltCam (mean α_{Camera} = 0.44, 95% credible intervals = −0.46 to 1.65) than the closed cod end (mean α_{Trawl} = −1.25, 95% credible intervals = −2.99 to 0.60, Table 1).

Objective 3

Simulations demonstrated that relative bias in all parameter estimates decreased as the number of tows increased, retention efficiency of both gear types increased, and the number of replicated passes increased (Figure 6; see also Appendix B, Figures B1–B5). Patterns in RMSE for all parameters and simulation scenarios showed that RMSE decreased with higher sample size, number of replicates, and greater retention efficiency of each gear type (Figure 7). For simplicity, we only present results for intercept (α) and slope (β) parameters for simulation scenarios that matched our observed data set (SmeltCam retention efficiency = 0.6, and trawl closed cod end retention efficiency = 0.4; Figure 7).

Parameter interval coverage was high among all scenarios (all parameters were covered by 95% credible intervals in at least 83% of simulations); consequently, we similarly only present interval coverage of intercept and slope parameters for the same scenarios as RMSE (Figure 7). Simulation results for scenarios similar to our observed field data (number of tows = 52 and 1 replicate) showed coverage to be greater than 93% for the intercept and slope parameters, and RMSE to be low for both parameters (RMSE < 0.14, Figure 7).

DISCUSSION

We presented a combined gear sampling design within an integrated analytical framework to demonstrate the potential of the SmeltCam as a valid sampling alternative to conventional closed cod-end trawling gears used in the estuary. By allowing combined gear deployment to act as sampling replicates (see Coggins Jr. et al. 2014), we were able to estimate the retention efficiency of each gear type. Simulations further demonstrated that the integrated model can provide unbiased parameter estimates as long as model assumptions are met, and sample sizes are—as they were in the present study—high enough. The combined gear sampling design and analytical framework implemented here provides evidence that the SmeltCam is as efficient as a conventional midwater trawl at detecting fish available to the gear.

We found observed fish counts from the SmeltCam to be similar to trawl counts, but this direct relationship was variable, and reflected the imperfect retention efficiency of each gear type. (Again, retention efficiency is the probability that a fish is detected once it is in contact with the gear.) Retention efficiency was estimated for both gear types in this study, and is a common component of catchability estimated in fisheries studies (Walsh 1997). Mitchell et al. (2017, 2019) used covered cod end and paired gear sampling methods for midwater trawling surveys within the estuary. These surveys were not 100% efficient at capturing Delta Smelt, and smaller fishes were less likely to be retained than larger fish. Although we did not directly
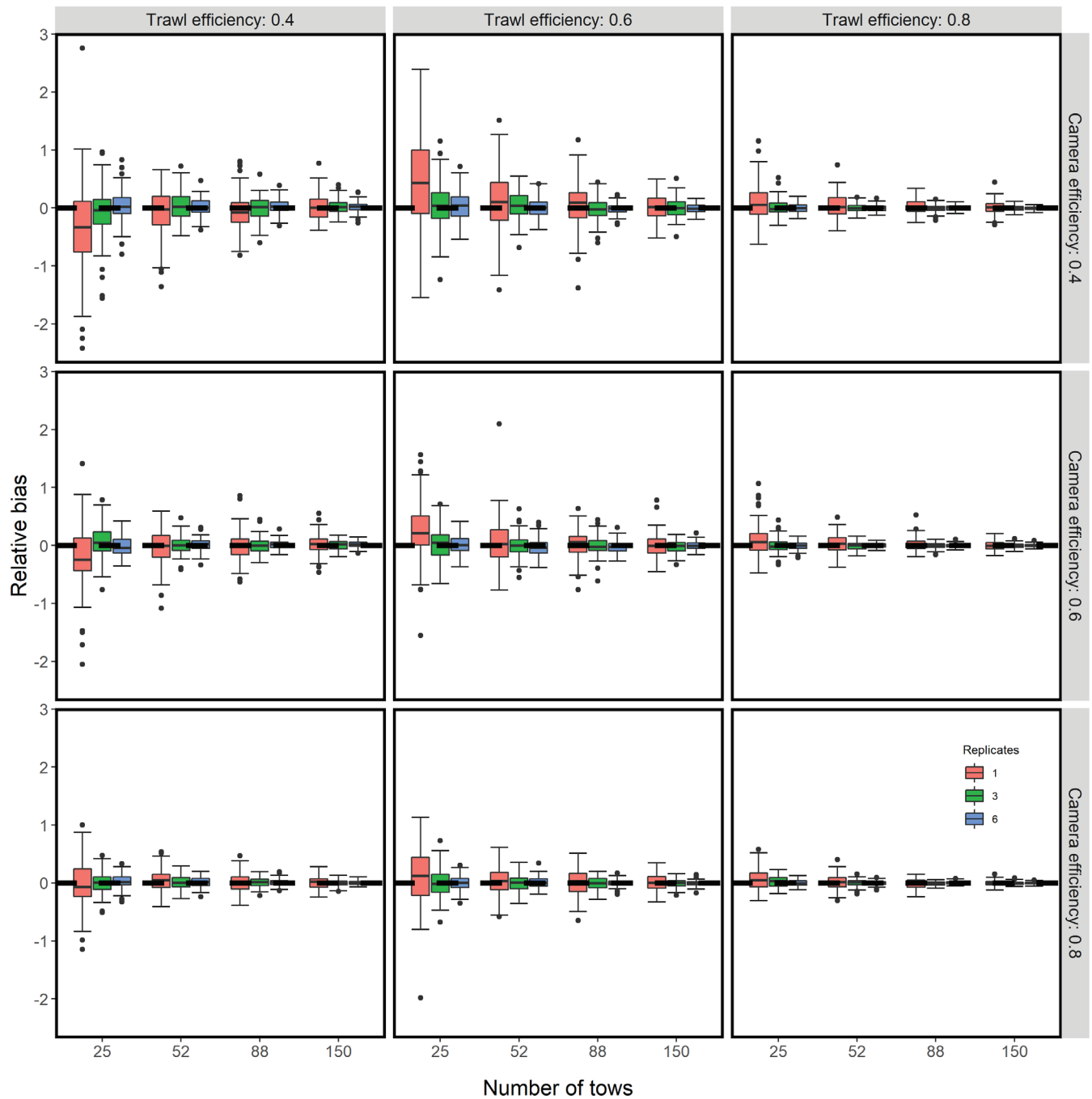
Figure 6 Relative bias for the SmeltCam retention efficiency intercept from simulations of the integrated binomial *N*-mixture model based on paired SmeltCam and closed cod-end sampling scenarios

test fish size during our surveys, fish size likely explains a considerable amount of variability in the retention efficiency estimates made for the trawl and the SmeltCam in our study. Fish size effects on retention efficiency estimates could be addressed with future modifications to the

SmeltCam by incorporating multiple camera mounts (pairs of stereo-imaging cameras) that would allow for fish sizes to be determined (Rosen et al. 2013; Williams et al. 2015; DeCelles et al. 2017).
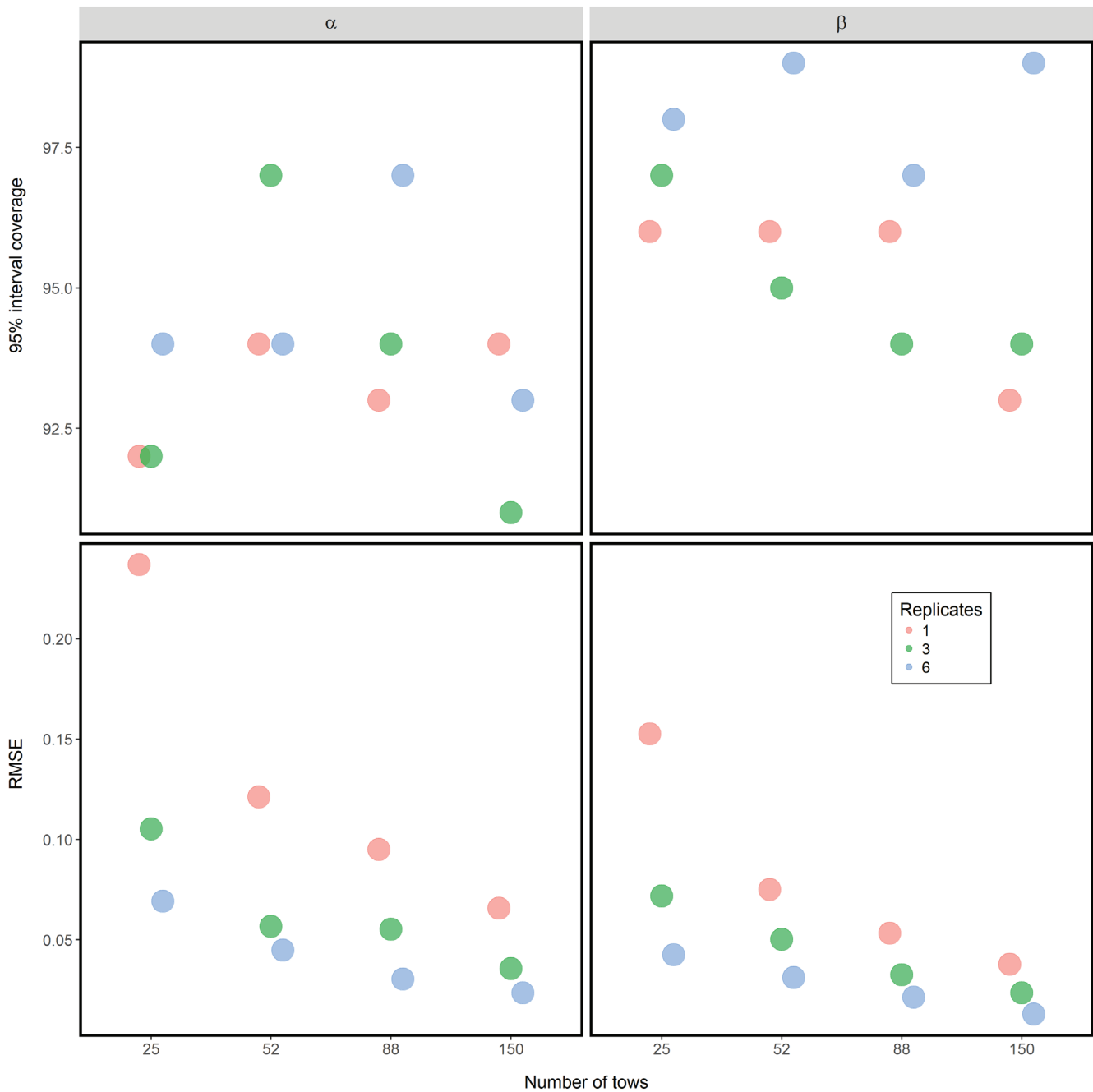
Figure 7 SmeltCam retention efficiency intercept (α) and slope (β) coefficient coverage by 95% credible intervals and root-mean-squared-error (RMSE) based on simulations of the integrated binomial *N*-mixture model. Interval coverage is the percent of 100 simulations in which the 95% credible intervals captured the true parameter value. Scenarios represented include the retention efficiency of the SmeltCam = 60%, retention efficiency of the closed cod end of the trawl = 40%, with all other simulation scenarios shown (different number of sites and number of true closed replicate passes).

The inclusion of covariates was important for our analyses because different aspects of sampling design can affect the efficiency by which gears perform. Turbidity was expected to negatively

affect our ability to detect fish with the SmeltCam, similar to issues encountered in other image sampling approaches (DeCelles et al. 2017). However, we could not confirm whether there was

a meaningful turbidity effect on the SmeltCam's performance. If turbidity is, in fact, important for SmeltCam performance, our analysis would indicate that our samples were not collected along a broad enough turbidity gradient (from 2.3 to 36.5 NTU) to detect an effect. We also included the total density of fish in the trawl as a factor affecting retention efficiency of the conventional trawling gear, and found evidence that the trawl was more efficient when fish densities were higher. Higher fish densities can fill mesh and prevent smaller fishes from escaping, a mechanism described for other trawling surveys in the estuary (Mitchell et al. 2017; Peterson and Barajas 2018).

The simultaneous deployment of the SmeltCam and closed cod-end midwater trawl was used to estimate gear retention efficiency for these gear types. Similar approaches have conceptually been taken in other studies, where cameras combined with other sampling gears (e.g., baited traps) are simultaneously deployed to estimate the same latent state variables (e.g., abundance, occupancy) using different gear types to inform the sampling efficiency of the complementary gear type (Bacheler et al. 2013; Kotwicki et al. 2013; Coggins Jr. et al. 2014). As expected, our simulations indicated greater accuracy and precision in parameter estimates when greater sample sizes and a greater number of closed-replicate passes were included (Zipkin et al. 2014; Duarte et al. 2018). However, increasing the number of true, closed replicate samples collected within the estuary to improve gear sampling efficiency is not a trivial matter, and cannot easily be addressed simply by increasing sampling effort. Confirming that sampling conditions are truly closed during replicate sampling passes is challenging, but is a requirement for estimating other decomposed forms of the detection process (e.g., the probability a fish is available to the sampling gear; Hostetter et al. 2019). For this study, we estimated the probability that a fish was retained by the sampling gear, but this value is conditional on a fish already being available to the sampling gear. Future efforts to reduce uncertainty in developing biological metrics from long-term trawling data sets in the estuary would greatly benefit from identifying sources of variability in detection efficiency beyond gear retention.

We used the binomial N-mixture model for our analysis, which can generate biased results if modeling assumptions are not met. First, the N-mixture model implicitly requires that double counting does not occur during data collection (Kéry 2018). The SmeltCam data could violate this assumption because a fish could move into or out of the scope of detection for the camera during a single tow. Similar counts between gears suggest that no strong violation of this assumption occurred during this study, but confirmation is not possible without unique fish identification. The N-mixture model also has issues with parameter identifiability when fit without covariate relationships in the observation or latent state processes ("intercept only models," Barker et al. 2018; Kéry 2018). However, we included covariate effects on both the observation and latent state processes, with strong covariate effects detected in the latter. Collectively, our results demonstrate that the SmeltCam provides abundance estimates that are as reliable as the conventional trawl, and can be used as a valid alternate sampling gear choice when monitoring at-risk populations such as the Delta Smelt.

ACKNOWLEDGEMENTS

or product names is for descriptive purposes only and does not imply endorsement by the US Government.

REFERENCES

Amundson CL, Royle JA, Handel CM. 2014. A hierarchical model combining distance sampling and time removal to estimate detection probability during avian point counts. Auk [accessed 2020 May 05];131(4):476–494. https://doi.org/10.1642/auk-14-11.1

Bacheler NM, Schobernd CM, Schobernd ZH, Mitchell WA, Berrane DJ, Kellison GT, Reichert MJM. 2013. Comparison of trap and underwater video gears for indexing reef fish presence and abundance in the southeast United States. Fish Res [accessed 2020 Jun 13];143:81–88. https://doi.org/10.1016/j.fishres.2013.01.013

Barker RJ, Schofield MR, Link WA, Sauer JR. 2018. On the reliability of N-mixture models for count data. Biometrics [accessed 2020 Jun 13];74(1):369–377. https://doi.org/10.1111/biom.12734

[CDFW] California Department of Fish and Wildlife. 2020. State and federally listed endangered and threatened animals of California. [accessed 2020 Jun 13]. Available from: https://nrm.dfg.ca.gov/FileHandler.ashx?DocumentID=109405&inline

Coggins Jr LG, Bacheler NM, Gwinn DC. 2014. Occupancy models for monitoring marine fish: a Bayesian hierarchical approach to model imperfect detection with a novel gear combination. PLoS ONE. [accessed 2020 Mar 20];9(9):1–14. https://doi.org/10.1371/journal.pone.0108302

DeCelles GR, Keiley EF, Lowery TM, Calabrese NM, Stokesbury KDE. 2017. Development of a video trawl survey system for New England Groundfish. Trans Am Fish Soc [accessed 2020 Apr 13];146(3):462–477. https://doi.org/10.1080/00028487.2017.1282888

Duarte A, Adams MJ, Peterson JT. 2018. Fitting N-mixture models to count data with unmodeled heterogeneity: bias, diagnostics, and alternative approaches. Ecol Modell [accessed 2020 May 22];374:51–59. https://doi.org/10.1016/j.ecolmodel.2018.02.007

Feyrer F, Nobriga ML, Sommer TR. 2007. Multidecadal trends for three declining fish species: habitat patterns and mechanisms in the San Francisco Estuary, California, USA. Can J Fish Aquat Sci [accessed 2020 Mar 20];64(4):723–734. https://doi.org/10.1139/F07-048

Feyrer F, Portz D, Odum D, Newman KB, Sommer T, Contreras D, Baxter R, Slater SB, Sereno D, van Nieuwenhuyse E. 2013. SmeltCam: underwater video codend for trawled nets with an application to the distribution of the imperiled Delta Smelt. PLoS ONE [accessed 2020 May 20];8(7). https://doi.org/10.1371/journal.pone.0067829

Feyrer F, Slater SB, Portz DE, Odom D, Morgan–King T, Brown LR. 2017. Pelagic nekton abundance and distribution in the northern Sacramento–San Joaquin Delta, California. Trans Am Fish Soc [accessed 2020 Mar 20];146(1):128–135. https://doi.org/10.1080/00028487.2016.1243577

Gelman A, Rubin DB. 1992. Inference from iterative simulation using multiple sequences. Stat Sci [accessed 2020 Mar 20];7:457–472. https://doi.org/10.1214/ss/1177011136

Graves TA, Kendall KC, Royle JA, Stetz JB, Macleod AC. 2011. Linking landscape characteristics to local grizzly bear abundance using multiple detection methods in a hierarchical model. Anim Conserv. [accessed 2020 Mar 20];14(6):652–664. https://doi.org/10.1111/j.1469-1795.2011.00471.x

Harrison XA. 2014. Using observation-level random effects to model overdispersion in count data in ecology and evolution. PeerJ [accessed 2020 Jun 19];2014(1). https://doi.org/10.7717/peerj.616

Hostetter NJ, Gardner B, Sillett TS, Pollock KH, Simons TR. 2019. An integrated model decomposing the components of detection probability and abundance in unmarked populations. Ecosphere [accessed 2020 Apr 23];10(3):e02586. https://doi.org/10.1002/ecs2.2586

Kellner K. 2019. JagsUI: A wrapper around "rjags" to streamline "JAGS" analyses. R package version 1.5.1. [accessed 2020 Mar 20]. Available from: https://CRAN.R-project.org/package=jagsUI

Kéry M. 2010. Introduction to WinBUGS for ecologists: Bayesian approach to regression, ANOVA, mixed models and related analyses. Burlington (MA): Academic Press. 320 p.

Kéry M, Royle JA. 2016. Applied hierarchical modeling in ecology: analysis of distribution, abundance and species richness in R and BUGS: Volume 1: Prelude and Static Models. Burlington (MA): Academic Press. 808 p.

Kéry M. 2018. Identifiability in N-mixture models: a large-scale screening test with bird data. Ecology [accessed 2020 Jun 13];99(2):281–288. https://doi.org/10.1002/ecy.2093

Kimmerer WJ, Rose KA. 2018. Individual-based modeling of Delta Smelt population dynamics in the upper San Francisco Estuary III. Effects of entrainment mortality and changes in prey. Trans Am Fish Soc [accessed 2020 Dec 11];147:223–243. https://doi.org/10.1002/tafs.10015

Kotwicki S, De Robertis A, Ianelli JN, Punt AE, Horne JK. 2013. Combining bottom trawl and acoustic data to model acoustic dead zone correction and bottom trawl efficiency parameters for semipelagic species. Can J Fish Aquat Sci [accessed 2020 Mar 10]; 70(2):208–219. https://doi.org/10.1139/cjfas-2012-0321

Makowski D, Ben–Shachar MS, Lüdecke D. 2019. bayestestR: describing effects and their uncertainty, existence and significance within the Bayesian framework. J Open Source Softw [accessed 2021 Jan 05];4(40):1541. https://doi.org/10.21105/joss.01541

Millar RB, Fryer RJ. 1999. Estimating the size-selection curves of towed gears, traps, nets and hooks. Rev Fish Biol Fish [accessed 2020 Mar 24];(1):89–116. https://doi.org/10.1023/A:1008838220001

Mitchell L, Newman K, Baxter R. 2017. A covered cod-end and tow-path evaluation of midwater trawl gear efficiency for catching Delta Smelt (*Hypomesus transpacificus*). San Franc Estuary Watershed Sci. [accessed 2020 Mar 06];15(4). https://doi.org/10.15447/sfews.2017v15iss4art3

Mitchell L, Newman K, Baxter R. 2019. Estimating the size selectivity of fishing trawls for a short-lived fish species. San Franc Estuary Watershed Sci [accessed 2020 Mar 06];17(1). https://doi.org/10.15447/sfews.2019v17iss1art5

Nichols JD, Thomas L, Conn PB. 2009. Inferences about landbird abundance from count data: recent advances and future directions. In: Thomson DL, Cooch EG, Conroy MJ, editors. Modeling demographic processes in marked populations. Boston (MA): Springer. [accessed 2020 May 27]; p. 201–235. Available from: https://doi.org/10.1007/978-0-387-78151-8

Peterson JT, Barajas MF. 2018. An evaluation of three fish surveys in the San Francisco Estuary, California, 1995–2015. San Franc Estuary Watershed Sci [accessed 2020 Apr 06];16(4). https://doi.org/10.15447/sfews.2018v16iss4art2

Plummer M. 2017. JAGS version 4.3.0 user manual. accessed 2021 May 22]. Available from: https://sourceforge.net/projects/mcmc-jags/

Polansky L, Mitchell L, Newman KB. 2019. Using multistage design-based methods to construct abundance indices and uncertainty measures for Delta Smelt. Trans Am Fish Soc [accessed 2020 Jan 14];148(4):710–724. https://doi.org/10.1002/tafs.10166

R Core Team. 2020. R: a language and environment for statistical computing. [accessed 2020 Jan 14]. R Vienna, Austria: Foundation for Statistical Computing. https://www.R-project.org/

Rosen S, Jörgensen T, Hammersland–White D, Holst JC. 2013. DeepVision: a stereo camera system provides highly accurate counts and lengths of fish passing inside a trawl. Can J Fish Aquat Sci [accessed 2020 Jun 23];70(10):1456–1467. https://doi.org/10.1139/cjfas-2013-0124

Royle JA. 2004. N-mixture models for estimating population size from spatially replicated counts. Biometrics [accessed 2020 Mar 06];60(1):108–115. https://doi.org/10.1111/j.0006-341X.2004.00142.x

Royle JA, Nichols JD, Kéry M. 2005. Modelling occurrence and abundance of species when detection is imperfect. Oikos [accessed 2020 Mar 20];110(2):353–359. https://doi.org/10.1111/j.0030-1299.2005.13534.x

Steinke DA, Young MJ, Feyrer FV. 2018. Vertical distribution of Longfin Smelt in the San Francisco Estuary. Version 2.1, August 2020. US Geological Survey data release. [accessed 2021 Feb 25]. Available from: https://doi.org/10.5066/F7SF2VF5

Vasilakopoulos P, Jardim E, Konrad C, Rihan D, Mannini A, Pinto C, Casey J, Mosqueira I, O'Neill FG. 2020. Selectivity metrics for fisheries management and advice. Fish Fish [accessed 2020 Apr 13];21:621–638. https://doi.org/10.1111/faf.12451

Walsh SJ. 1997. Efficiency of bottom sampling trawls in deriving survey abundance indices. NAFO Sci Counc Stud [accessed 2020 Mar 10];28:9–24. https://doi.org/10.1016/S0967-0653(97)85803-6

Walther BA, Moore JL. 2005. The concepts of bias, precision and accuracy, and their use in testing the performance of species richness estimators, with a literature review of estimator performance. Ecography [accessed 2020 Apr 23];28:815–829. https://doi.org/10.1111/j.2005.0906-7590.04112.x

Williams K, Horne JK, Punt AE. 2015. Examining influences of environmental, trawl gear, and fish population factors on midwater trawl performance using acoustic methods. Fish Res [accessed 2020 Mar 09];164:94–101. https://doi.org/10.1016/j.fishres.2014.11.001

Zhao Q, Royle JA. 2019. Dynamic N-mixture models with temporal variability in detection probability. Ecol Modell [accessed 2020 Apr 23];393:20–24. https://doi.org/10.1016/j.ecolmodel.2018.12.007

Zhou S, Klaer NL, Daley RM, Zhu Z, Fuller M, Smith ADM. 2014. Modelling multiple fishing gear efficiencies and abundance for aggregated populations using fishery or survey data. ICES J Mar Sci [accessed 2020 Apr 15];71(9):2436–2447. https://doi.org/10.1093/icesjms/fsu068

Zipkin EF, Thorson JT, See K, Lynch HJ, Grant EHC, Kanno Y, Chandler RB, Letcher BH, Royle JA. 2014. Modeling structured population dynamics using data from unmarked individuals. Ecology [accessed 2020 Mar 20];95(1):22–29. https://doi.org/10.1890/13-1131.1